International Journal of Mechanical and Industrial Engineering

Volume 1 | Issue 1 Article 11

July 2011

Experimental Investigation on the Effect of Multi-Winglets

Srikanth G,
Hindustan University, Chennai, India, srikanthaero@yahoo.com

Surendra Bogadi
Hindustan University, Chennai, India, aero.academic@gmail.com

Experimental Investigation on the Effect of Multi-Winglets

[1]Srikanth G, [2]Surendra Bogadi
[1]*PG Scholar; Dept. of Aeronautical Engineering,* [2]*Asst.Professor; Dept. of Aeronautical Engineering*
[1,2]*Hindustan University, Chennai, India*
E-mail : srikanthaero@yahoo.com, aero.academic@gmail.com

***Abstract*—An extensive experimental study is conducted to examine the potentiality of Multi-Winglets (similar to bird tip feathers) for the reduction of Induced Drag, improved C_L without increase in span of aircraft wing. The model composed of a rectangular wing built from NACA 0015 airfoil constituted of three winglets, which are small wings without sweep & twist. The test conducted in subsonic wind tunnel at flow speed 20m/s and placing the wing at angle of attack ranging from -5 to +15 deg. And also the wing with no winglet (bare wing) and with single winglet also tested in the same condition as in the case of three winglets (multi-winglet). Wind tunnel balances provided lift measurements and tuft flow visualization obtained wingtip vortex information. The results show that multi-winglet system reduced induced drag by 27.9% and improved C_L by 26.5% compare to bare wing.**

Keywords-Induced drag;multi-winglet;

NOMENCLATURE

C_L	Coefficient of Lift
C_{Di}	Coefficient of Induced Drag
α	Angle of Attack
AR	Aspect Ratio
e	Span Effeciency Factor
WWNW	Wing with No Winglet
WWSW	Wing with Single Winglet
WWMW	Wing with Multi-Winglet

I. INTRODUCTION

Ever since man started to think about flying, has striven to imitate the shape and structure of a bird wing. The researchers began to look at the flying characteristics of soaring birds such as eagles, hawks, condors, vultures, and ospreys. Each of these birds has wings with "pin" feathers at the ends that produce slotted wingtips. They found that the pin feathers worked to reduce drag, as well as being used to provide roll control, in the same manner as ailerons on aircraft.

The requirements of many modern aircraft missions are such that high values of aerodynamic efficiency must be obtained with aircraft having wings of relatively restricted span lengths. In many of these missions the aircraft must operate at relatively large values of the lift coefficient, and the large induced drag associated with the small span consequently results in a rather low value for the operational aerodynamic efficiency. In endeavoring to increase the flight efficiency of such aircraft, it becomes necessary to investigate more complex and unconventional wing forms which might offer the possibility of securing appreciable reductions in the induced drag, subject to the restriction of limited span length. Such forms are to be found among the various non-planar lifting systems in which the lifting surfaces (wings) have an appreciable curvature or extension in a vertical/horizontal plane perpendicular to the direction of flight called Winglets.

The vortices produced at the wing –tips are unavoidable products by the lift presence, so it means the difficulties due to force that support the aircraft in the air. These vortices are responsible for the appearance of Induced Drag.

In cruise conditions the induced drag is responsible for approximately 30% on entire drag and also 50% in high-lift conditions [1]. Hence to reduce the induced drag, winglets are been used, by
which fuel consumption goes down and range is extended, may achieve better lift.

Richard T Whitcomb [2] invented the Winglets in the early 1970's as a means by which wing lift-to-drag performance could be increased. Indeed, his research in 1976 indicated that winglets could reduce induced drag by twenty percent, resulting in about nine percent better lift-to-drag performance at 0.78 Mach for a specified wing loading. In the early days of the winglet era, only business jets adopted winglets, mostly due to aesthetic reasons. It shows the drag reduction [3] for the Gulfstream III, one of the pioneer corporate aircraft to adopt winglets. The flight test conducted at Mach number of 0.75 indicates a greater drag reduction than the wind tunnel test had indicated. M. J. Smith et al [4-6] effort examined the potential of multi-winglets for the reduction of induced drag without increasing the span of aircraft wings. A redefinition of multiple winglet configurations is proposed by U. La Roche and H.L. La Rochein [7] order to understand and facilitate exploiting the massive induced drag reductions of streamwise staggered multiple winglets, which, using the Prandtl-Munk vortex sheet model.

II. EXPERIMENTAL CONFIGURATION

Experiments have been carried out in the subsonic wind tunnel facility available at the Aerodynamics Laboratory of Hindustan University, which has a test section size of 600 mm x 600 mm x 2000 mm. at flow velocity 20 & 28m/s and angles of attack ranging from -5 to +15 degree.

Evaluation of the induced drag effects was made using the standard equation,

$$C_{Di} = \frac{C_L^2}{\pi e AR}$$

Where aspect ratio (AR) =4, and *e* is approximately 0.94 for WWNW and 0.907 for WWSW [8].
And e = 1.125 for WWMW-A and 0.9534 for WWMW-B [9]

III. MODEL DESCRIPTION

The wing model used in the study made of Teak wood has chord of 75mm and semi span of 300mm with 42 pressure ports, 21 on upper and 21 on lower surface as shown in Fig.(1,2)

The single winglet has 75mm chord at bottom and taper ratio is 0.3. The each regime in multi-winglet has chord of 54mm, taper ratio of 1 and angle between each regime is 30degree shown in Fig (3-6).

IV. RESULTS AND DISCUSSIONS

The qualitative and quantitative experiments conducted in the present study are tufts flow visualization and force measurements respectively.

A. Force measurements;

Forces of various wing/winglets combinations, as shown in Table 1 to 4, were evaluated to determine the combination that provided the best improvement in lift-to-drag ratio (L/D_i), C_L

C_L increase as α increased, for WWSW C_L increases with α up to 7 degree, after that it is decreased. For WWMW-A, C_L increased with Angle of Attack (α) up to 10degree and in the case of WWMW-B, C_L falls at 12 degree Angle of Attack (α).

At Angle of Attack (α) = -5degree, the maximum negative lift coefficient produced for WWMW-B followed by WWMW-A, WWSW, WWNW. At α =0 degree multi-winglet system could not make positive lift.

At α =5,7 degree $(C_L)_{max}$ observed in single winglet system by 13.52 and 20% respectively compare to WWNW. But at high angles of attack (above 10 deg.) $(C_L)_{max}$ observed in multi-winglet system up to 26.5% as shown in Fig.(8)

L/D_i is maximum at low Angles of Attack for Multi-Winglet configurations and especially more better for WWMW-A and L/D_i is maximum at high Angles of Attack (10deg and above) for WWSW as shown in Fig (9)

And maximum reduction in induced drag is for WWMW-A about 27.9 and 15% at α =5 and 7 degree respectively.

Fig (10) gives the clear picture of variation of C_{Di} and C_L for all the modes with respect to angle of attack.

B. Tufts Flow Visualization;

In order to recognize the wing flow pattern tufts are attached over the wing surface. Tufts flow visualization at $\alpha=0^0$, all tufts are fully attached to the surface, no movement of tufts are observed for all the models.

Fig.11-13, shows the tufts flow visualization at $\alpha=5^0$, where a slight movement of tufts is observed in the WWNW and no movement for WWMW-A & B, which means slight unsteadiness is present for bare wing but not for wing with multi-winglet systems.

Fig.14-19, shows for $\alpha=10^0$ and 15^0, here the complete disturbing and fluttering of tufts are observed for all the models, indicates unsteadiness in the flow because of the formation of vortices but it is observed more disturbance for WWNW and slightly for WWMW-B and less in the case of WWMW-A.

Hence it concluded that WWMW-A performance better in reducing the vortices, hence the induced drag.

V. CONCLUSIONS

Experiments have been performed to examine the potentiality of multiple winglets mounted at varying cant/toe angles to improve the aerodynamic characteristics of a wing in subsonic flow. Combining the force measurement results with the flow visualization some conclusions are drawn;

1) Stall angle for Multi-Winglet system is much higher than Single Winglet system.

2) At low angles of attack Single Winglet system produces better C_L compare to Multi-Winglet system.

3) At high angles of attack Multi-Winglet system produces better C_L.

4) L/D is high at low angles of attack for Multi-Winglet system (up to 7 deg.).

5) Multi-Winglets can reduce Induced drag in more percentage compare to Single Winglet system at low angles of attack.

6) Among the two Multi-Winglets configurations WWMW-A is better than WWMW-B in overall performance

ACKNOWLEDGMENT

The present work has been carried in Department of Aeronautical Engineering, Hindustan University. The authors would like to express their appreciation to the HOD for his support.

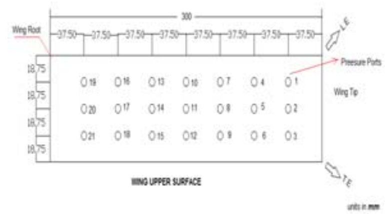

Figure 1. Wing Upper Surface; Pressure port Arrangements

REFERENCES

[1] *F.M.Catalona et al., "Experimental Analysis of Aerodynamics Characteristics of Adaptive Multi-Winglets," presented at 24th International Congress of the Aeronautical Sciences,2004.*

[2] *Richard Whitcomb, "A Design Approach and Selected Wind-Tunnel Results at High Subsonic Speeds for Wing-Tip Mounted Winglets," NASA TN D-8260, July.*

[3] *Bento S.de Mattos et al., "Considerations about Winglet Design," AIAA 2003-3502, 2003*

[4] *M.J.Smith et al., "Performance Analysis of a Wing with Multiple Winglets," AIAA 2001-2407*

[5] *Ilan Kroo, John et al., "Highly Non planar Lifting Systems," Presented at: Transportation Beyond 2000: Technologies Needed for Engineering Design, NASA Langley Research Center, September 26-28, 1995*

[6] *Mohammad Reza Soltani et al., "Experimental investigation of the effect of various winglet shapes on the total pressure distribution behind a wing," presented at 24th international congress of the aeronautical sciences,2004*

[7] *U.La Roche and H.L.La Roche., "Induced drag reduction using Multi-Winglets, looking beyond the Prandtl-Munk Linear Model." AIAA 2004-2120.*

[8] *Daniel P.Raymer., "Aircraft Design: A Conceptual Approach," Fourth Edition, Published by AIAA*

[9] *Vorgelegt Von et al., "Potential of Multi-Winglet Systems to Improve Aircraft Performance", D83, Berlin 2008*

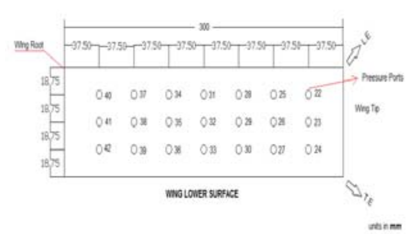

Figure 2. Wing Lower Surface; Pressure port Arrangements

Figure 3. Photograph of WWNW (top view)

Figure 4. Photograph of WWSW (front view)

Figure 5. Photograph of WWMW-A

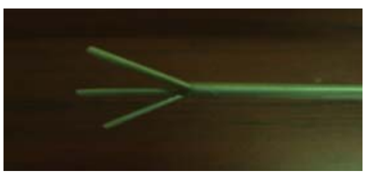

Figure 6. Photograph of WWMW-B (front view)

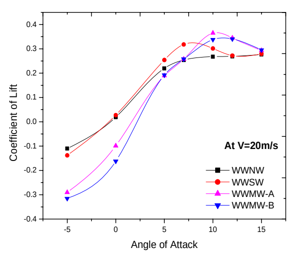

Figure 7. Comparison Curve; Coefficient of Lift (C_L) vs Angle of Attack (α) in degree

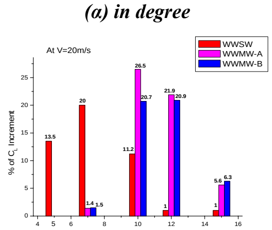

Figure 8. Angle of Attack (α) vs % of C_L increment over WWNW

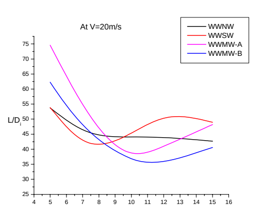

Figure 9. Comparison of L/D_i at various angles of attack

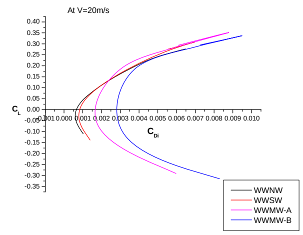

Figure 10. Curve C_L vs C_{Di}

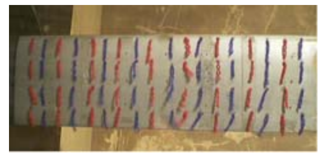

Figure 11. Tufts flow visualization for WWNW at α = 5deg

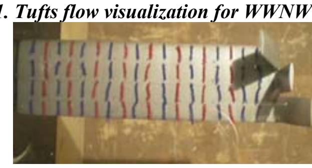

Figure 12. Tufts flow visualization for WWMW-A at α = 5deg

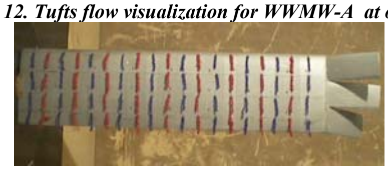

Figure 13.Tufts flow visualization for WWMW-B at α = 5deg

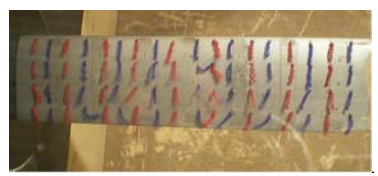

Figure 14. Tufts flow visualization for WWNW at α = 10deg

Figure 15. Tufts flow visualization for WWMW-A at α = 10deg

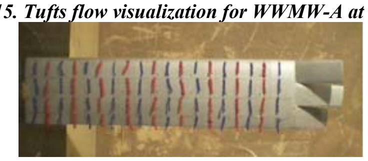

Figure 16. Tufts flow visualization for WWMW-B at α = 10deg

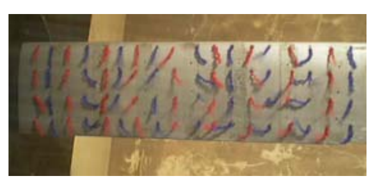

Figure 17. Tufts flow visualization for WWNW at α = 15deg.

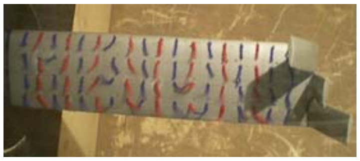

Figure 18. Tufts flow visualization for WWMW-A at α = 15deg.

Table 1 Force measurement for WWNW

α in degree	C_L	C_{Di}	L/D_i
-5	-0.10989	0.001023	107.41
0	0.01923	0.00003131	614.18
5	0.21978	0.0040892	53.746
7	0.25412	0.0054668	46.484
10	0.26786	0.0060741	44.098
12	0.26923	0.0061364	43.874
15	0.27679	0.0064858	42.676

Table 2 Force measurement for WWSW

α in degree	C_L	C_{Di}	L/D_i
-5	-0.13805	0.001393	-99.107
0	0.02748	0.0000552	497.8787
5	0.25412	0.00472	53.839
7	0.3180	0.007391	43.024
10	0.30151	0.006645	45.377
7	0.25824	0.0055663	46.393
10	0.33791	0.00953053	35.455
12	0.34066	0.0096863	35.169
15	0.29533	0.0072799	40.567

12	0.27197	0.005406	50.306
15	0.27953	0.005711	48.945

Figure 19. Tufts flow visualization for WWMW-B at α = 15deg.

Table 3 Force measurement for WWMW-A

α in degree	C_L	C_{Di}	L/D_i
-5	-0.29052	0.00597021	-48.661
0	-0.0989	0.00069188	-142.943
5	0.18956	0.00254174	74.578
7	0.25756	0.0046924	54.888
10	0.3647	0.0094083	38.763
12	0.34478	0.0084086	41.003
15	0.29326	0.0060834	48.206

Table 4 Force measurement for WWMW-B

α in degree	C_L	C_{Di}	L/D_i
-5	-0.31525	0.0082952	-38.003
0	-0.16209	0.0021929	-73.915
5	0.1923	0.00308655	62.302